



Ultra-short DBR fiber laser with high-temperature resistance using tilted fiber Bragg grating output coupler

XUANTUNG PHAM,^{1,2} JINHAI SI,^{1,*} TAO CHEN,¹ ZHEN NIU,¹
FENGQIN HUANG,¹ AND XUN HOU¹

¹Key Laboratory for Physical Electronics and Devices of the Ministry of Education & Shaanxi Key Lab of Information Photonic Technique, School of Electronics & Information Engineering, Xi'an Jiaotong University, No. 28, Xianning West Road, Xi'an, 710049, China

²Le Quy Don Technical University, Hanoi 122314, Vietnam

*jinhaisi@mail.xjtu.edu.cn

Abstract: We demonstrate a high-temperature resistant distributed Bragg reflector (DBR) fiber laser that is highly compact with an entire cavity length of 12 mm. A partial-reflection tilted fiber Bragg grating (PR-TFBG) is used as the laser output coupler whose reflectivity can be adjusted by changing the TFBG tilt angle. The laser cavity consists of two strong gratings including the PR-TFBG and a high-reflection fiber Bragg grating (HR-FBG), which is directly fabricated in an Er-doped fiber using a femtosecond laser and a phase mask. The thermal stability of the PR-TFBG and HR-FBG is experimentally investigated. After an annealing process, their remained gratings are stable at high temperatures and strong enough for laser oscillation. The laser is also annealed before its stability is tested. The results show that the laser can stably operate in single longitudinal mode with a signal-to-noise ratio better than 65 dB over the temperature range from room temperature to 550°C.

© 2019 Optical Society of America under the terms of the [OSA Open Access Publishing Agreement](#)

1. Introduction

A distributed Bragg reflector (DBR) fiber laser has attracted considerable interest in the field of single-frequency fiber lasers and optical fiber sensors due to its advantages in compactness, high sensing resolution, and high signal-to-noise ratio (SNR) as well as multiplexing capability [1–5]. The DBR laser cavity is comprised of a pair of narrowband fiber Bragg gratings (FBGs) with a short piece of rare-earth-doped fiber. The narrowband FBGs generally include a high-reflection FBG (HR-FBG) and a partial-reflection FBG (PR-FBG) based laser output coupler (OC) [1]. A regular DBR fiber laser can hardly operate in high-temperature environments resulting from the thermal degradation of its consisted FBGs. Since the thermal stability of the FBGs determines that of the formed DBR fiber laser, DBR fiber lasers based on the FBGs with high-temperature resistance have been fabricated [6–8]. Y. Lai *et al.* have demonstrated a DBR fiber laser with a cavity length of 31 mm which was fabricated in an Er/Yb co-doped fiber using a femtosecond laser and point-by-point technique [6]. This DBR fiber laser can operate at 600°C. B. Guan *et al.* have fabricated highly saturated Bragg gratings in an Er/Yb co-doped fiber and formed a DBR laser with a cavity length of 25 mm which can be stable at 500°C [7]. Moreover, a DBR laser that can survive at high temperatures up to 750°C has been formed by splicing an Er-doped silica fiber to a pair of regenerated FBGs inscribed in hydrogen loaded single-mode fiber (SMF-28) [8]. Since the regenerated FBG had relatively low reflectivity, a long active fiber of 150 mm was required to provide sufficient gain for the laser oscillation, reducing the laser compactness. Recently, several high-temperature resistant DBR fiber lasers with ultra-short cavity lengths have been presented for applications requiring high spatial resolution sensors [9,10]. Ran *et al.* have reported an ultra-short DBR fiber laser with a cavity length of 13 mm which was constructed

by using a pair of type IIa FBGs [9]. The laser can withstand a high temperature of 600°C. H. Wang *et al.* have realized an ultra-short DBR Yb-doped fiber laser based on type Ia FBGs [10]. The laser with an entire cavity length of 10 mm can steadily operate at 450°C. However, since ultraviolet lasers were used as fabrication light sources in these works, a highly photosensitive active fiber or a hydrogen-loaded process was demanded. The long exposure times of around 40 minutes and 8 minutes were also required to fabricate the type Ia and IIa FBGs, respectively.

A partial-reflection OC of the DBR fiber laser is generally obtained by tailoring the grating strength or grating length of the FBG [7–9,11,12]. For the method of controlling the FBG grating strength, the OC commonly has a slightly weaker or even the same grating strength compared with the HR-FBG to ensure that the Bragg wavelength and thermal stability of these two gratings can be the same [8,9,11]. In this case, the reflectivities of the OC and HR-FBG are almost identical, resulting in the low laser threshold as well as low output power. B. Guan directly fabricated FBGs with different grating lengths (reflectivities) in the active fiber using a 193 nm excimer laser with a phase mask and the beam scanning technique, in which the phase mask and fiber were fixed while the laser beam scanned along the fiber [7,12]. The PR-FBG and HR-FBG were written with the same beam scanning speed so that they had the same grating strength, thereby the same Bragg wavelength as well as thermal stability. Since the beam scanning speed was slow (20 $\mu\text{m/s}$), a relatively long time was required to fabricate an FBG with a grating length of around 10 mm. The FBGs with different grating lengths can also be fabricated using a femtosecond laser with the point-by-point technique and the required exposure time is highly shortened [6,13]. While this method is very flexible, it requires a high accuracy positioning system. Recently, we have proposed a tilted FBG (TFBG) fabrication method using a femtosecond laser and a phase mask, in which the tilted grating planes were obtained by obliquely scanning the fiber while the laser beam and phase mask were fixed [14]. Using this fabrication method, the Bragg wavelengths of the TFBGs with different tilt angles were identical and can match well with that of a regular FBG. Importantly, the TFBG was stable at temperatures up to 700°C, and its reflectivity decreased with the increasing tilt angle [14–16]. Thus, a TFBG with the desired reflectivity can be obtained and used as the OC of the fiber laser with high-temperature resistance.

In this paper, we present a high-temperature resistant DBR fiber laser that possesses an ultra-short cavity with an entire length of 12 mm. The laser uses a partial-reflection TFBG (PR-TFBG) as the OC whose reflectivity can flexibly be adjusted by changing the TFBG tilt angle. To form the laser cavity, a pair of strong gratings including the PR-TFBG and an HR-FBG is directly fabricated in a commercial available Er-doped fiber using a femtosecond laser and a phase mask. The PR-TFBG and HR-FBG are experimentally investigated in terms of their thermal responses. After an annealing process at 600°C for 5 hours, the reflectivities of their remained gratings are stable at high temperatures and sufficient for laser oscillation. The laser is also annealed at 600°C for 5 hours before its stability is tested at various temperatures. The results show that the laser can stably operate in single longitudinal mode with an SNR better than 65 dB at high temperatures up to 550°C. The results provide a novel structure of the DBR fiber laser that is capable of stable operating in extreme circumstances and open a potential application of TFBGs as the OC in fiber lasers.

2. Experimental setup

In our experiments, all the gratings were fabricated in a commercial available Er-doped fiber (Liekki Er80-8/125, manufactured by nLight Inc., Finland) which has a core diameter of 8 μm and a cladding diameter of 125 μm . The peak absorption at 976 nm was measured to be 25 dB/m. The numerical aperture of the active fiber is 0.13. An amplified Ti: sapphire laser (Libra-USP-HE, Coherent Inc., USA) generates femtosecond laser pulses with a center wavelength of 800 nm, pulse duration of 50 fs, and a repetition rate of 1 kHz. The 12 mm diameter laser beam with 600- μJ pulse energy was focused using a cylindrical lens (focal length of 25 mm) through a

second-order phase mask (pitch of 2.142 μm) into the active fiber. The fiber was placed 3 mm away from the phase mask to generate pure interference between ± 1 st-order diffractive laser beams. The second-order phase mask was used here instead of a first-order one (pitch of 1.071 μm) is because higher-order phase masks have better zero-order suppression of the diffractive beams, eliminating the influence of the zero-order on the interference pattern [17]. The detailed TFBG fabrication method that can also use for the FBG fabrication was demonstrated in our previous report [14]. The Bragg resonance λ_B of both the TFBG and FBG appears at a wavelength that meets the phase-matching condition given by $m\lambda_B = 2n_{\text{eff}}\Lambda_g$, where m is the harmonic order number, n_{eff} is the effective index of the guided mode at λ_B , and Λ_g is the grating period along the fiber axial direction [17,18]. With the fabrication condition in our experiments, the fabricated gratings were corresponding to type I-IR gratings as the white light generation that is coincident with type II-IR grating formation was not observed during the laser irradiation [19]. This type I-IR grating can survive at temperatures below 700°C [14,19]. The grating periods along the fiber axial direction of the FBG and TFBGs with different tilt angles were all the same and could be given by $\Lambda_g = \Lambda_m/2$, where Λ_m is the pitch of the phase mask [14]. Here, since the phase mask with the pitch of 2.142 μm was used, the Bragg resonance of around 1550 nm was corresponding to the second harmonic resonance ($m = 2$). During the fabrication process, a broadband source (BBS) with a wavelength range of 1520-1580 nm and an optical spectrum analyzer (OSA) (Yokogawa, AQ6370D) with a spectral resolution of 0.02 nm were used to monitor and record the grating transmission spectrum.

The ultra-short DBR fiber laser was fabricated by directly writing a pair of strong gratings including an HR-FBG and a PR-TFBG based OC in the Er-doped fiber as shown in Fig. 1. Here, the HR-FBG and PR-TFBG were fabricated in the same conditions to ensure the consistency of their thermal responses, thereby the laser stability at different temperatures. A 976 nm laser diode (LD) was used as a pump source, which is coupled into the laser cavity through a 980/1550 nm wavelength division multiplexer (WDM).

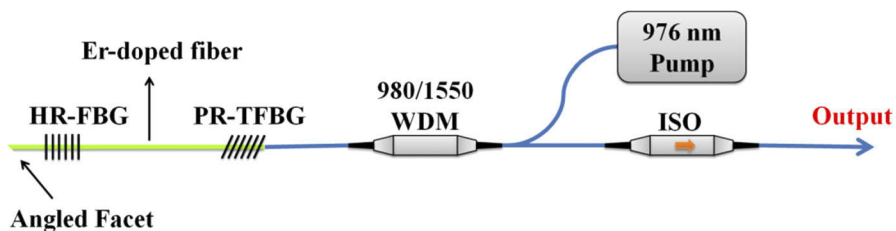


Fig. 1. Experimental setup of the ultra-short DBR fiber laser.

3. Results and discussions

3.1. Fabrications of the PR-TFBG and HR-FBG in Er-doped fiber and their thermal responses

We fabricated several gratings including an FBG (0° TFBG) and TFBGs with tilt angles from 1.8° to 3.8° in the Er-doped fiber. The transmission spectra of these gratings are shown in Fig. 2(a). In the fabrication process, the exposure times to obtain strong gratings with saturated reflectivities were 40 s and from 45 s to 60 s for the FBG and TFBGs, respectively. The grating lengths of these gratings were the same and measured to be 5 mm. The grating periods along the axial direction of these gratings were 1.07 μm which is half of the phase mask pitch. As can be seen in Fig. 2(a), the Bragg resonances of the TFBGs with different tilt angles match well with that of the FBG. The FBG possesses a high reflectivity of over 40 dB ($> 99.99\%$) and is highly suited to use as the HR-FBG in the laser cavity. As the tilt angle of the TFBG increases, its

reflectivity decreases and is 28.5 dB, 14.5 dB, 8.2 dB, and 5.3 dB for the 1.8°, 2.5°, 3.0°, and 3.8° TFBGs, respectively. These results indicate that a strong TFBG with different reflectivities can be obtained by changing its tilt angle and is capable of using as the OC that meets the requirement in various kinds of fiber lasers [12,20,21].

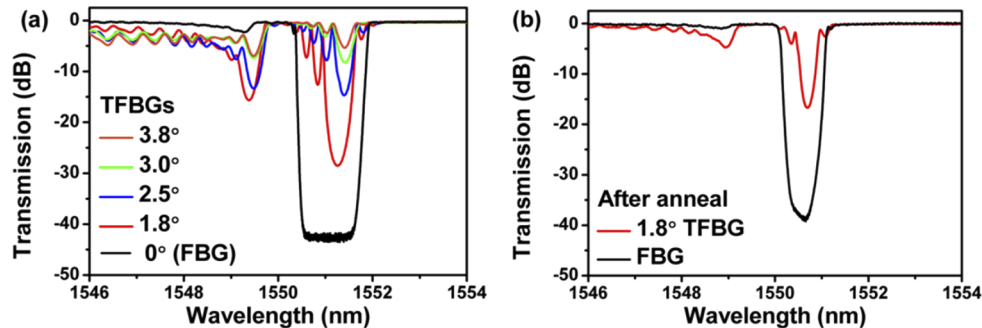


Fig. 2. (a) The transmission spectra of the TFBGs with tilt angles from 0° to 3.8°. The 0° TFBG is also a regular FBG. (b) The transmission spectra of the 1.8° TFBG and FBG after the annealing process. These transmission spectra are measured at room temperature (28°C).

The FBG and 1.8° TFBG were selected to investigate their thermal responses. These two gratings were put into a tube oven and annealed at 600°C for 5 hours. This tube oven can provide good control of the temperature with an accuracy of $\pm 1^\circ\text{C}$ at temperatures from 300°C to 1200°C. The transmission spectra of the remained FBG and 1.8° TFBG after the annealing process are shown in Fig. 2(b). The Bragg wavelengths of these gratings shift to the short-wavelength side resulting from the grating degradation in the annealing process. The remained FBG and 1.8° TFBG still possess high reflectivities which are approximately 38.0 dB and 16.5 dB. Furthermore, the bandwidths significantly decrease from 1.52 nm to 0.98 nm for the FBG and from 1.10 to 0.64 nm for the 1.8° TFBG, respectively.

Subsequently, these two gratings were tested at temperatures from 300°C to 800°C to investigate the consistency of their thermal responses. At temperatures below 500°C, the test duration was set to 30 min to stabilize the temperature in the tube oven and obtain stable spectra. At temperatures above 500°C, this duration was set to a longer time of 2 hours to further study the thermal stability of these two gratings. Figures 3(a) and 3(b) show the measured Bragg wavelengths of the 1.8° TFBG and FBG in response to temperature variations. The transmission spectra of these gratings at various temperatures are shown in insets of Figs. 3(a) and 3(b). The Bragg wavelengths of these gratings shift to the long-wavelength side as the temperature increases. Here, the good linear relationships (regression coefficients of over 99.9%) between the Bragg wavelength and temperature are obtained at temperatures from 300°C to 800°C for both the 1.8° TFBG and FBG with similar sensitivities of 15.05 pm/°C and 15.41 pm/°C, respectively. The Bragg wavelengths of these gratings at room temperature deviate from the linear fitting lines. This is because of the low sensitivity of the fabricated gratings in the low-temperature region which is similar to that of the grating reported in [22].

The reflectivity stabilities of the 1.8° TFBG and FBG at temperatures from 300°C to 800°C are shown in Figs. 3(c) and 3(d), respectively. At temperatures from 300°C to 600°C, no obvious degradation in the TFBG reflectivity is observed. At temperatures of 700°C and 800°C, the TFBG reflectivity decreases as shown in Fig. 3(c). As shown in Fig. 3(d), the FBG shows no obvious degradations with the reflectivity of over 36.5 dB at temperatures from 300°C to 600°C. At temperatures of 700°C and 800°C, the FBG reflectivity decreases sharply, which is consistent with that of the TFBG. At temperatures from 300°C to 600°C, it can also be observed that the FBG reflectivity is higher at temperatures of 350°C, 400°C, and 600°C than at other

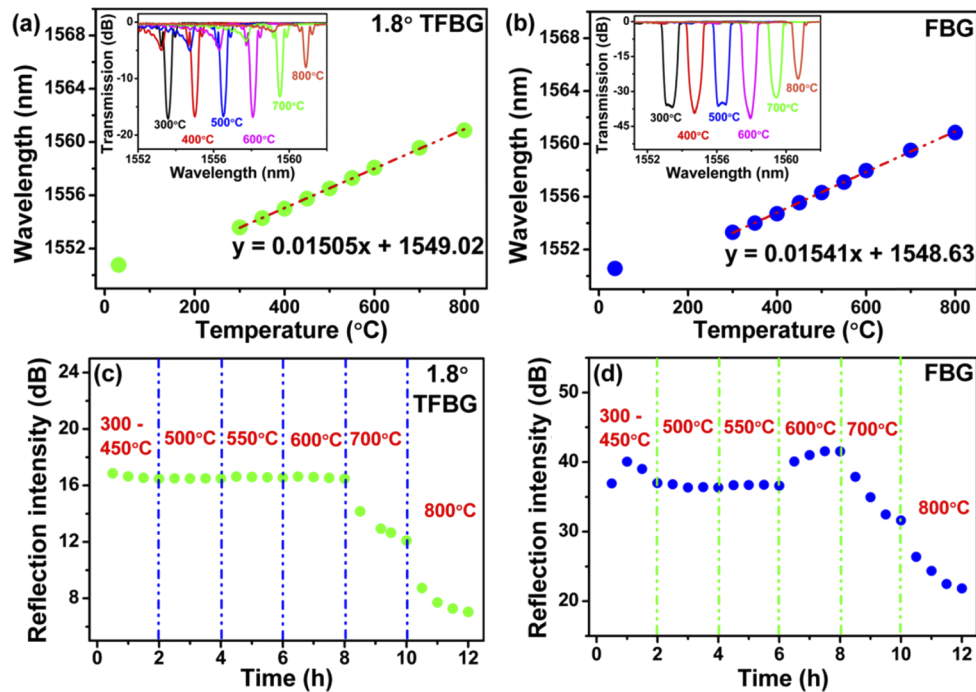


Fig. 3. The Bragg wavelengths of the (a) 1.8° TFBR and (b) FBG versus temperature. The insets show the transmission spectra of the 1.8° TFBR and FBG at various temperatures. Thermal stability of the (c) 1.8° TFBR and (d) FBG at temperatures from 300°C to 800°C after the annealing process.

temperatures. This situation only occurs in the case of the FBG with high reflectivity. The reason for this could be contributed to the influence of the fluorescence in the active fiber which is pumped by the BBS. Here, the reflectivities of the FBG and TFBR were obtained by measuring their Bragg resonance transmissivities. As the FBG possesses high reflectivity, the transmitted intensity of the BBS at the FBG Bragg resonance is weak and could even be comparative with the fluorescence intensity. In this case, the variation of the fluorescence intensity that is caused by the two following reasons can result in the fluctuation of the measured transmissivity (reflectivity) at the FBG Bragg resonance. First, according to the gain spectrum of the Er-doped fiber, the fluorescence intensity at the Bragg resonance changes according to the redshift of the Bragg resonance as the temperature increases. Second, it was demonstrated that the gain in the Er-doped fiber that determines the fluorescence intensity decreases as the temperature increases [23]. This phenomenon can be observed from the shape of the FBG Bragg resonance at different temperatures as shown in the inset of Fig. 3(b). In contrast, since the TFBR has a much lower reflectivity than that of the FBG, the transmitted intensity of the BBS at its Bragg resonance is greatly higher than the fluorescence intensity. Thus, the influence of the fluorescence intensity variation on the TFBR transmissivity at different temperatures is negligible. Besides, the FBG reflectivity slightly increases from about 40 dB to 41.5 dB (less than 0.01%) during the testing time of 2 hours at 600°C. A possible explanation for this is that the fabricated gratings have some defects that suppress the grating reflectivity. When the temperature increases to 600°C, these defects may be slowly decayed, thereby increasing the grating reflectivity. Nevertheless, since this effect is extremely weak, it can only be observed when the transmitted intensity of the BBS is weak, e.g., the case of the FBG with high reflectivity.

The above results suggest that after the annealing process, the FBG and 1.8° TFBG still possess high reflectivities and are stable at high temperatures up to 600°C . It also appears that these gratings are consistent in their thermal responses including temperature sensitivity and thermal stability. As a result, these gratings could potentially be used to form a DBR fiber laser that may stably operate at 600°C .

3.2. Fabrication of the DBR fiber laser and its thermal response

Considering the grating degradation in the annealing process and the limited gain of the ultra-short cavity of the formed DBR fiber laser, the 1.8° TFBG with the relatively high reflectivity was used as the OC. This ensures that even after the grating degradation at elevated temperatures, the remained grating can still be strong enough for the laser oscillation. The 1.8° TFBG and FBG spaced 2 mm apart were directly fabricated in the Er-doped fiber to form the laser cavity, and the total exposure time took around 90 s. The fabrication condition of these two gratings was the same as those gratings mentioned in the previous section. The grating lengths of the 1.8° TFBG and FBG were measured to be 5 mm, making the entire cavity length of 12 mm. Figure 4(a) shows the image of the laser, in which the fiber section with green fluorescence is the laser cavity. The spectra of the laser cavity and laser output at a pump power of 255 mW are shown in Fig. 4(b). Several superimposed resonances are observed, each of which corresponds to a longitudinal mode, indicating the effect of a Fabry-Perot cavity. The laser operates in two longitudinal modes because it possesses a wide-bandwidth OC of around 1.10 nm as described previously. In this case, the output power of each longitudinal mode is unstable as the mode competition occurs. The longitudinal mode space is approximately 0.21 nm, corresponding to an effective cavity length of 4 mm.

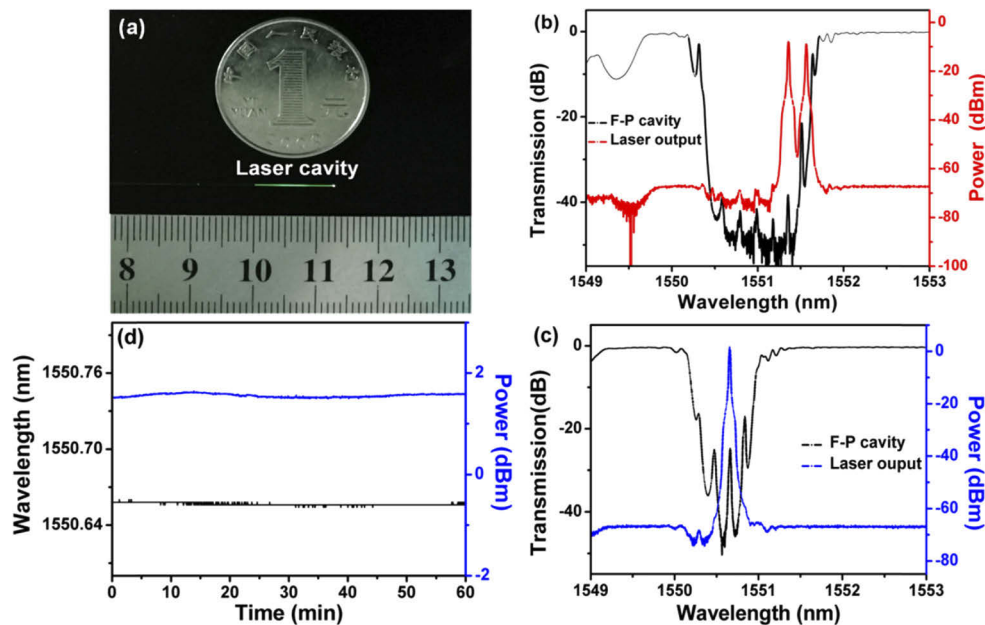


Fig. 4. (a) Photograph of the DBR fiber laser. The transmission spectra of the F-P interference and the output spectra of the laser (b) before and (c) after the annealing process. The pump power of 255 mW is used. (d) The stability of the laser output power and wavelength at room temperature in 1 hour.

Subsequently, the fabricated DBR fiber laser was annealed at 600°C for 5 hours. After the annealing process, the lasing threshold increases from 10 mW to 16 mW, resulting from

the grating degradations. The spectra of the laser cavity and laser output at the pump power of 255 mW were re-measured and are shown in Fig. 4(c). It can be observed that the laser cavity bandwidth narrows down significantly from 1.49 nm to 0.86 nm. The number of strong superimposed resonances decreases from six to three. Particularly, the laser operates in single longitudinal mode with an SNR of over 65 dB, as shown in Fig. 4(c). The laser short-term stability at room temperature of 28°C was tested for 1 hour (1800 samples were recorded), and the results are shown in Fig. 4(d). The lasing wavelength is highly stable at a wavelength of 1550.66 nm with a standard deviation smaller than 0.02 nm. The average power of the laser output is 1.556 dBm with a standard deviation of approximately 0.032. These results indicate that the DBR fiber laser operates stably in single longitudinal mode at room temperature after the annealing process.

Next, the performance of the DBR fiber laser was tested at temperatures from 300°C to 650°C. The test duration at temperatures below 500°C was set to 30 min to stabilize the temperature in the tube oven and obtain stable spectra. This duration was set to 3 hours at temperatures from 500°C to 600°C and 1 hour at 650°C to investigate the laser thermal stability. As shown in Fig. 5(a), the lasing wavelength shifts linearly to the long-wavelength side with a sensitivity of 15.13 pm/°C as the temperature increases from 300°C to 650°C. This sensitivity agrees well with those of the gratings described previously. The laser operates in single longitudinal mode at temperatures from 300°C to 650°C as shown in the inset of Fig. 5(a). The SNR of the laser output is better than 65 dB at temperatures from 300°C to 550°C.

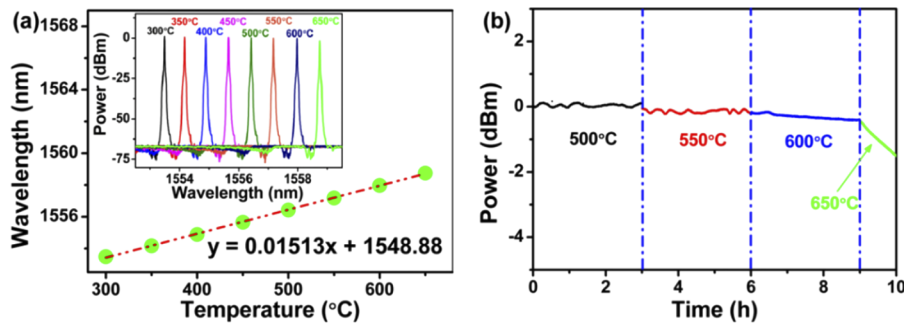


Fig. 5. (a) The lasing wavelength versus temperature. The inset shows the output spectra of the DBR laser at different temperatures. (b) Laser output power stability at different temperatures.

Figure 5(b) shows the stability of the laser output power at temperatures from 500°C to 650°C. At temperatures of 500°C and 550°C, the laser output power is highly stable without any degradation over the whole duration of 6 h. At 500°C, the average power of the laser output is 0.036 dBm with a standard deviation of 0.041. At 550°C, it is -0.146 dBm with a standard deviation of 0.046. These fluctuations are small and comparable to that at room temperature, indicating the stable operation of the laser at high temperatures up to 550°C. It can be observed that the laser output powers are different at room temperature, 500°C, and 550°C, respectively. The reason for this could be that the gain in Er-doped fiber at the lasing wavelength changes according to the variation of the temperature as well as lasing wavelength [23]. At temperatures of 600°C and 650°C, the laser output power linearly degrades with degradation rates of 0.083 dBm and 1.049 dBm per hour, respectively. From these results, it can be summarized that after the annealing process, the DBR fiber laser can stably operate in single longitudinal mode with an SNR of over 65 dB at high temperatures up to 550°C. This high thermal resistance of the fabricated laser is comparative with that of the one based on the type IIa Bragg gratings whose SNR is only around 44 dB [9]. The thermal resistance of the DBR fiber laser could be further

improved by using the type II-IR gratings that can withstand temperatures above 1000°C [19,24]. Nevertheless, since the type II-IR gratings have relatively high insertion loss, a long or high gain coefficient active fiber is required to provide sufficient gain for the laser oscillation.

4. Conclusion

We demonstrate a high-temperature resistant DBR fiber laser whose cavity is ultra-short with an entire length of 12 mm. The laser OC is a PR-TFBBG whose reflectivity can be tailored by changing the TFBBG tilt angle. The laser cavity consists of a pair of strong gratings including the PR-TFBBG and an HR-TFBBG, which is directly fabricated in Er-doped fiber using a femtosecond laser and a phase mask. After an annealing process, the fabricated gratings and laser are all stable at high temperatures. The laser can stably operate in single longitudinal mode with an SNR better than 65 dB at high temperatures up to 550°C.

Funding

National Key Research and Development Program of China (2017YFB1104600); Key Research and Development Program of Shaanxi Province (2017ZDXM-GY-120); Fundamental Research Funds for the Central Universities (XJJ2016016).

Disclosures

The authors declare no conflicts of interest.

References

1. S. Fu, W. Shi, Y. Feng, L. Zhang, Z. Yang, S. Xu, X. Zhu, R. A. Norwood, and N. Peyghambarian, "Review of recent progress on single-frequency fiber lasers," *J. Opt. Soc. Am. B* **34**(3), A49 (2017).
2. Y. Zhang, B. Guan, and H. Tam, "Characteristics of the distributed Bragg reflector fiber laser sensor for lateral force measurement," *Opt. Commun.* **281**(18), 4619–4622 (2008).
3. Y. Zhang and B. Guan, "High-Sensitivity Distributed Bragg Reflector Fiber Laser Displacement Sensor," *IEEE Photonics Technol. Lett.* **21**(5), 280–282 (2009).
4. W. Liu, T. Guo, A. C. Wong, H. Y. Tam, and S. He, "Highly sensitive bending sensor based on Er³⁺-doped DBR fiber laser," *Opt. Express* **18**(17), 17834–17840 (2010).
5. Y. Zha, Z. Xu, P. Xiao, F. Feng, Y. Ran, and B. Guan, "Phase-shifted type-IIa fiber Bragg gratings for high-temperature laser applications," *Opt. Express* **27**(4), 4346–4353 (2019).
6. Y. Lai, A. Martinez, I. Khrushchev, and I. Bennion, "Distributed Bragg reflector fiber laser fabricated by femtosecond laser inscription," *Opt. Lett.* **31**(11), 1672–1674 (2006).
7. B. Guan, Y. Zhang, H. Wang, D. Chen, and H. Tam, "High-temperature-resistant distributed Bragg reflector fiber laser written in Er/Yb co-doped fiber," *Opt. Express* **16**(5), 2958–2964 (2008).
8. R. Chen, A. Yan, M. Li, T. Chen, Q. Wang, J. Canning, K. Cook, and K. P. Chen, "Regenerated distributed Bragg reflector fiber lasers for high-temperature operation," *Opt. Lett.* **38**(14), 2490–2492 (2013).
9. Y. Ran, F. Feng, Y. Liang, L. Jin, and B. Guan, "Type IIa Bragg grating based ultra-short DBR fiber laser with high temperature resistance," *Opt. Lett.* **40**(24), 5706–5709 (2015).
10. H. Wang, S. Xiong, J. Song, F. Zhao, Z. Yan, X. Hong, T. Zhang, W. Zhang, K. Zhou, C. Li, and Y. Wang, "High temperature resistant ultra-short DBR Yb-doped fiber laser," *Appl. Opt.* **58**(16), 4474–4478 (2019).
11. F. Feng, Y. Ran, Y. Liang, S. Gao, Y. Feng, L. Jin, and B. Guan, "Thermally triggered fiber lasers based on secondary-type-In Bragg gratings," *Opt. Lett.* **41**(11), 2470–2473 (2016).
12. Y. Zhang, B. O. Guan, and H. Y. Tam, "Ultra-short distributed Bragg reflector fiber laser for sensing applications," *Opt. Express* **17**(12), 10050–10055 (2009).
13. Y. Lai, K. Zhou, K. Sugden, and I. Bennion, "Point-by-point inscription of first-order fiber Bragg grating for C-band applications," *Opt. Express* **15**(26), 18318–18325 (2007).
14. R. Wang, J. Si, T. Chen, L. Yan, H. Cao, X. Pham, and X. Hou, "Fabrication of high-temperature tilted fiber Bragg gratings using a femtosecond laser," *Opt. Express* **25**(20), 23684–23689 (2017).
15. X. Pham, J. Si, T. Chen, R. Wang, L. Yan, H. Cao, and X. Hou, "Demodulation method for tilted fiber Bragg grating refractometer with high sensitivity," *J. Appl. Phys.* **123**(17), 174501 (2018).
16. X. Pham, J. Si, T. Chen, F. Qin, and X. Hou, "Wide Range Refractive Index Measurement Based on Off-Axis Tilted Fiber Bragg Gratings Fabricated Using Femtosecond Laser," *J. Lightwave Technol.* **37**(13), 3027–3034 (2019).

17. S. J. Mihailov, C. W. Smelser, D. Grobnc, R. B. Walker, P. Lu, H. Ding, and J. Unruh, "Bragg Gratings Written in All-SiO₂ and Ge-Doped Core Fibers With 800-nm Femtosecond Radiation and a Phase Mask," *J. Lightwave Technol.* **22**(1), 94–100 (2004).
18. X. Zhang, C. Chen, Y. Yu, W. Wei, Q. Guo, Y. Chen, X. Zhang, L. Qin, Y. Ning, and H. Sun, "High-Order-Tilted Fiber Bragg Gratings With Superposed Refractive Index Modulation," *IEEE Photonics J.* **10**(1), 1–8 (2018).
19. C. Smelser, S. Mihailov, and D. Grobnc, "Formation of Type I-IR and Type II-IR gratings with an ultrafast IR laser and a phase mask," *Opt. Express* **13**(14), 5377–5386 (2005).
20. S. H. Xu, Z. M. Yang, T. Liu, W. N. Zhang, Z. M. Feng, Q. Y. Zhang, and Z. H. Jiang, "An efficient compact 300 mW narrow-linewidth single frequency fiber laser at 1.5 μm ," *Opt. Express* **18**(2), 1249–1254 (2010).
21. Q. Fang, J. Li, W. Shi, Y. Qin, Y. Xu, X. Meng, R. A. Norwood, and N. Peyghambarian, "5 kW Near-Diffraction-Limited and 8 kW High-Brightness Monolithic Continuous Wave Fiber Lasers Directly Pumped by Laser Diodes," *IEEE Photonics J.* **9**(5), 1–7 (2017).
22. T. Wang, L. Shao, J. Canning, and K. Cook, "Temperature and strain characterization of regenerated gratings," *Opt. Lett.* **38**(3), 247–249 (2013).
23. N. Kagi, A. Oyobe, and K. Nakamura, "Temperature dependence of the gain in erbium-doped fibers," *J. Lightwave Technol.* **9**(2), 261–265 (1991).
24. F. Huang, T. Chen, J. Si, X. Pham, and X. Hou, "Fiber laser based on a fiber Bragg grating and its application in high-temperature sensing," *Opt. Commun.* **452**, 233–237 (2019).